Nucleation by Free Radicals from the Photooxidation of Sulfur Dioxide in Air

James P. Friend,* Robert A. Barnes, and Rita M. Vasta

Department of Chemistry, Drexel University, Philadelphia, Pennsylvania 19104 (Received: August 16, 1979; In Final Form: April 11, 1980)

Previously reported experimental results of the production of condensation nuclei by the photooxidation of SO_2 in air are reanalyzed on the basis that the principal photochemical reaction of SO_2 is $SO_2 + OH + M \rightarrow HSO_3 + M$. The ideas that gaseous H_2SO_4 is the end product of the reaction and that nuclei were formed from clusters of H_2SO_4 and H_2O molecules are shown to be probably incorrect on the basis of (a) comparison to nucleation rates expected from the theory of heteromolecular homogeneous nucleation and (b) calculations indicating that nucleation rates were kinetically controlled such that the nuclei formed contained only one or two sulfur-bearing entities. The nucleation phenomena are compatible with the idea that free radicals and the hydrated complex $SO_3 \cdot H_2O$ are nuclei precursors. We suggest a mechanism involving the formation and recombination of hydrated forms of HSO_3 and HSO_5 radicals to explain nucleation for conditions of relative humidity greater than about 5%. For lower relative humidities the reaction $SO_2 + O + M \rightarrow SO_3 + M$ followed by the formation of a hydrated complex of SO_3 is suggested as controlling nucleation. A model based on these mechanisms yields the results that nuclei consist of single molecules of $H_2S_2O_6$ or possibly $H_2S_2O_8$, plus their associated H_2O molecules, at high relative humidities (>5%) and that at low relative humidities the nuclei consist of single molecules of H_2SO_4, plus associated H_2O molecules. These mechanisms are used as a basis for suggesting a general explanation for the phenomenon of photoinduced nucleation.

I. Introduction

The production of particles by photooxidation of sulfur dioxide has, for several years, been recognized as an important atmospheric process. The desire to understand details of the process has led to considerable experimentation under a variety of conditions.[1-8] In attempting to explain experimental observations, most workers have assumed that H_2SO_4 vapor is formed as a product of SO_2 photooxidation and that particles may form from clusters of H_2SO_4 and H_2O molecules. The chemical mechanisms of H_2SO_4 formation have been thought to proceed either by way of reaction of excited SO_2 with O_2,[5,7] as originally proposed by Blacet,[9] or via the reaction of SO_2 with O atoms.[2-4]

Most recently Marvin and Reiss[8] have reported on the gas-phase photooxidation of SO_2 in a diffusion cloud chamber with a gas phase consisting of He, H_2O vapor, and SO_2 (with SO_2 partial pressures on the order of a few torr). Oxygen was not present in their experiments, and the oxidation of SO_2 was attributed primarily to the disproportionation reaction between SO_2 and $SO_2(^3B_1)$ to yield SO_3 and SO. The observed nucleation was attributed to the interactions of H_2O with H_2SO_4 following rapid reaction of H_2O with SO_3. The disproportionation reaction was assumed to be the rate-determining step in H_2SO_4 production.

The present work is based upon the reanalysis of previously published data[3,4] in the light of the apparent importance of the reaction of OH with SO_2. The experimental system contained O_2, and O_3 was formed by irradiation of the system in the ultraviolet. The rate coefficient for the reaction of SO_2 with OH radicals has been measured by Davis et al.[10] and Castlemen et al.[11] The new results, in the form of nucleation rates, are compared with theoretical nucleation rates for gaseous mixtures of H_2SO_4 and H_2O as presented by Shugard and Reiss.[12] Large differences between the experiments and theory, in addition to the observed dependency of nucleation rates upon H_2O vapor pressure, are interpreted as indicating the possibility that nucleation is controlled by the reactions of hydrated free radicals and hydrated SO_3.

A discussion of reported experimental work of other investigators in nucleation is given in subsections F and G of the Discussion section in order to compare and illuminate further the results of the present work.

II. Background

A. Experiment. The experimental equipment and the results obtained in studies of the photooxidation of sulfur dioxide in air in the presence of water vapor have been described in two previous publications.[3,4] The equipment consisted basically of a laminar flow reactor into which trace quantities of gases (in this case SO_2, H_2O, and sometimes O_3) were introduced in known and controlled concentrations. Also, light in the near-ultraviolet and visible regions was introduced through windows in a direction perpendicular to the flow. Particles formed in the reactor were detected by using an Environment One condensation nuclei (CN) counter. Among the results of the previous work were the following:

a. Detectable particle formation did not occur when SO_2 was absent nor when it was present without a source of free radicals.

b. The quantum yield for the reaction sequence $SO_2 + h\nu \rightarrow SO_2^* + O_2 \rightarrow$ oxidation products was shown to be less than 10^{-9}, and it was concluded that this sequence is unimportant as an atmospheric process. The reanalysis of the photochemistry given in this paper does not alter this conclusion.

c. The relationship between nuclei formation and H_2O vapor concentrations was established in a series of experiments in which SO_2 concentrations and light intensity were held constant while varying H_2O vapor pressures.

Figure 1 shows the results of these experiments. This corresponds to Figure 6 in Leifer et al.,[4] except that the CN concentrations in Leifer et al.[4] have been transformed to nucleation rates. The error bars represent the estimated 30% uncertainty in the measured concentration of condensation nuclei.[46] Even without further analysis the sudden change in slope of the nucleation rate–H_2O vapor pressure curve in the vicinity of $p_{H_2O} = 1.5$ torr (6% relative humidity) is remarkable. The distribution of experimental points shown in Figure 1 indicates that the experimental findings are closely reproducible. A new analysis of these results requires examination of the photochemical processes occurring in the reactor, which in turn requires a

0022-3654/80/2084-2423$01.00/0

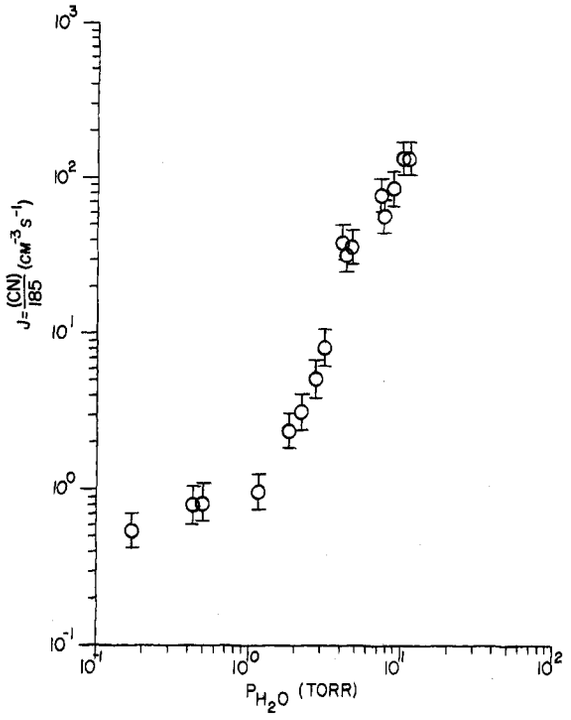

Figure 1. Observed nucleation rates vs. H_2O pressure based upon Leifer et al.[4] The nucleation rate J is the observed concentration of CN divided by the residence time (=185 s) in the nucleation zone of the reactor. The error bars correspond to a ±30% uncertainty in the measured CN concentration.

knowledge of the irradiance in the reactor as a function of wavelength. Values of this quantity are given in Table I for wavelength increments of 10 nm in the region of interest (where ozone and oxygen absorb to produce O atoms). Interpretations of the results originally centered around the idea that SO_2 was mainly oxidized to SO_3 by O atoms and the SO_3 reacted with water to form H_2SO_4 that further combined with water molecules to form nuclei. Leifer et al.[4] compared the interpreted results of Friend et al.[3] with theoretical calculations and concluded that there were large discrepancies between them. A discussion of our present ideas of the chemical processes in the reactor and our interpretation of the former results in the light of them are given below after a discussion of the theory of homogeneous heteromolecular nucleation.

B. Binary Nucleation Theory. Recently several papers have appeared treating the phenomenon of heteromolecular homogeneous nucleation (cf. Shugard and Reiss,[12] Kiang and Stauffer,[13] Hoppel,[14] Heist and Reiss,[15] and Mirabel and Katz[16]). The theory gives a thermodynamic treatment of mixtures of two types of gaseous molecules which, when associated with each other, can form a condensed phase that is also a mixture or a composite of the two types of molecules. The equilibrium vapor pressures in the composite condensed phase are lower than for the respective gases over the pure liquids (or solids). For sulfuric acid and water molecules the differences in vapor pressure are particularly large because of the large excess of free energy of mixing in the liquid phase. The papers referenced above all treat this problem. Details will not be given here. The interested reader is referred to Mirabel and Katz[16] for a clear presentation of the basic concepts and informative graphical results. The papers of Shugard et al.[17] and Shugard and Reiss[12] show how the theory is modified to account for the existence of hydrates of H_2SO_4 in vapor phase. Shugard and Reiss[12] have also presented a stochastic model which gives insight into transient as well as steady-state nucleation phenomena.

TABLE I: Experimental Irradiances, Filter Transmissivities, and Relevant Molecular Cross Sections Used in Calculating Photochemical Effects

wave-length interval, nm	$10^{-11} \cdot I(\lambda)$,[a] photon cm^{-2} s^{-1}	$T(\lambda)$,[b] %	$\sigma(\lambda)$,[c] cm^2	$\sigma(\lambda)$,[d] cm^2
200-205	0.69	0.0	1.23×10^{-23}	3.32×10^{-19}
205-210	0.78	0.0	1.01×10^{-23}	4.46×10^{-19}
210-215	0.91	0.0	8.70×10^{-24}	7.74×10^{-19}
215-220	1.11	0.0	7.10×10^{-24}	1.40×10^{-18}
220-225	1.48	5.7	4.90×10^{-24}	2.37×10^{-18}
225-230	2.03	19.2	3.35×10^{-24}	3.73×10^{-18}
230-235	3.20	35.7	2.50×10^{-24}	5.41×10^{-18}
235-240	4.92	52.1	1.40×10^{-24}	7.23×10^{-18}
240-245	5.97	63.7	0.50×10^{-24}	9.05×10^{-18}
245-250	6.95	71.0	0.0	1.05×10^{-17}
250-260	115	77.0	0.0	1.13×10^{-17}
260-270	797	80.6	0.0	9.71×10^{-18}
270-280	706	83.1	0.0	5.69×10^{-18}
280-290	1340	85.2	0.0	2.44×10^{-18}
290-300	1960	86.3	0.0	7.87×10^{-19}
300-310	1240	87.0	0.0	2.16×10^{-19}
310-320	1720	87.6	0.0	5.97×10^{-20}

[a] Irradiance. [b] Filter transmissivity. [c] O_2 absorption cross section. [d] O_3 absorption cross section.

For the purposes of the present paper the following features of the theory are noteworthy:

a. The steady-state nucleation rate of a binary system is given by

$$J = F \exp(-\Delta G^*/kT)$$

F is a frequency factor, ΔG^* is the free energy of formation of the embryonic nucleus (which is considered to be in unstable equilibrium with the gas phase), k is Boltzmann's constant, and T is the absolute temperature.

b. The steady-state theory permits evaluation of F and ΔG^* for any gas composition, that is, for any proportion of the two components. It considers that collisions and associations among the molecules occur to form clusters which are generally unstable. A fraction of the associations result in the formation of embryos of critical size above which the embryos become stable nuclei. For a given composition of the gas phase, the free energy of formation of embryos increases with the size of the cluster until a maximum is reached corresponding to the critical nucleus. Beyond that, the addition of molecules decreases the free energy of formation. The critical nuclei contain approximately 13 molecules of H_2SO_4 at a mole fraction of the order of 0.2 for 50% relative humidity, and they contain three molecules of H_2SO_4 at a mole fraction of 0.03 for 300% relative humidity (see ref 13). At equilibrium the ratio of the rate of binary collisions of H_2SO_4 molecules, Z_{AA}, to the nucleation rate, J, ranges from 10^{12} to 10^{17} depending on relative humidity.

c. The values of ΔG^* depend upon various thermodynamic quantities, for example, the partial molar volumes of the components of the liquid phase, the surface tension of the droplets (embryos), and the equilibrium vapor pressures of the pure components (at temperature T). The sensitivity of the nulceation rate to variations in these quantities is described by Mirabel and Katz[16] and by Hamill et al.[18] (see also Mirabel and Clavelin,[19] who have provided experimental verification of binary homogeneous nucleation theory). One of the major uncertainties for H_2SO_4 is the vapor pressure of the pure liquid at and below room temperature. The value used by recent workers is that calculated by Gmitro and Vermeulen[20] using van't Hoff's equation along with the heat capacity, standard heats of formation, standard entropies of formation, and

TABLE II: Photochemical Reactions in Experiment

no.	eq	symbol	photolysis rates and rate constants	ref
1	$O_2 + h\nu \rightarrow O(^3P) + O(^3P)$	j_1	1.01×10^{-12} s^{-1}	a
2	$O + O_2 + M \rightarrow O_3 + M$	k_2	5.92×10^{-34} cm^6 molecule^{-2} s^{-1}	b
3	$O_3 + h\nu \rightarrow O_2 + O(^1D)$	j_3	1.50×10^{-3} s^{-1}	a
4	$O_3 + h\nu \rightarrow O_2 + O(^3P)$	j_4	9.00×10^{-6} s^{-1}	a
5	$O(^1D) + M \rightarrow O(^3P) + M$	k_5	3.02×10^{-11} cm^3 molecule^{-1} s^{-1}	26
6	$O(^1D) + H_2O \rightarrow 2OH$	k_6	2.30×10^{-10} cm^3 molecule^{-1} s^{-1}	26
7	$SO_2 + OH + M \rightarrow HSO_3 + M$	k_7	2.30×10^{-32} cm^6 molecule^{-2} s^{-1}	11
8	$SO_2 + O + M \rightarrow SO_3 + M$	k_8	7.67×19^{-34} cm^6 molecule^{-2} s^{-1}	28
9	$HO_2 + SO_2 \rightarrow SO_3 + OH$	k_9	9.00×10^{-16} cm^3 molecule^{-1} s^{-1}	28
10	$OH + O_3 \rightarrow HO_2 + O_2$	k_{10}	5.23×10^{-14} cm^3 molecule^{-1} s^{-1}	26
11	$HO_2 + OH \rightarrow H_2O + O_2$	k_{11}	5.10×10^{-11} cm^3 molecule^{-1} s^{-1}	29

Experimental Conditions

$(M) = 2.46 \times 10^{19}$ molecules cm^{-3}
$(O_2) = 5.16 \times 10^{18}$ molecules cm^{-3}
$(SO_2) = 2.64 \times 10^{13}$ molecules cm^{-3} (=1.0 ppm)
$T = 298$ K

[a] Calculated for experimental conditions given in Table I. $j_1 = \Sigma_{\lambda_b}{}^{\lambda_a} \Phi(\lambda) I(\lambda) T(\lambda)$ where Φ is the quantum yield for the particular process considered; I and σ are the intensities and absorption cross sections relevant to the wavelength interval as listed in Table I. The factor T is the fractional transmissivity of the UG-5 filter used in the experiment. For ozone photolysis $\Phi(O(^3P))$ is considered to be unity for wavelengths greater than 310 nm, and $\Phi(O(^1D))$ is unity for λ less than 310 nm. For the photolysis of molecular oxygen the quantum yield of $O(^3P)$ is unity for 200 nm $< \lambda <$ 245.4 nm. [b] Reference 27. The value of the rate coefficient is the average of the values reported for N_2 and O_2 as third bodies, weighted according to atmospheric abundance.

the heat of vaporization of H_2SO_4 at 298 K. The value obtained is $p^e_{H_2SO_4} = 3.6 \times 10^{-4}$ torr. Verhoff and Banchero[21] have criticized the use of $p^e_{H_2SO_4}$ calculated by Gmitro and Vermeulen,[20] pointing out that the calculation is very sensitive to the standard enthalpy of formation of H_2SO_4 liquid and that the small experimental errors in the standard enthalpies and entropies (of the gas and the liquid) could lead to errors in the predicted sulfuric acid vapor pressure of several hundred percent.

Recent measurements of Chu and Morrison[22] of the equilibrium vapor pressure of H_2SO_4 at 298 K using a vapor effusion technique yield a value for $p^e_{H_2SO_4}$ of 3.1×10^{-5} torr. This is slightly more than an order of magnitude smaller than the value calculated by Gmitro and Vermeulen.[20] Figure 3 shows a set of theoretical nucleation rates plotted vs. activity using the measured value for $p^e_{H_2SO_4}$ of 3.1×10^{-5} torr for various relative humidities. The dashed curve on the right represents the theoretical nucleation rates for 50% relative humidity using $p^e_{H_2SO_4}$ equal to 3.6×10^{-4} torr (Gmitro and Vermeulen[20]). It is simply displaced upward by the ratio of the two vapor pressures.

III. Reanalysis of Results

The realization that the photochemical processes occurring in the reactor were quite different from those previously supposed prompted us to construct the list of equations given in Table II, which we believe properly represent the reaction system. Qualitatively, the process of nuclei precursor formation resulted from the following sequence:

a. Oxygen was photolyzed to form ground-state O atoms $O(^3P)$ (eq 1).

$$O_2 + h\nu \rightarrow O(^3P) + O(^3P) \quad (1)$$

b. Ozone was formed by the reaction of O atoms with oxygen (eq 2).

$$O + O_2 + M \rightarrow O_3 + M \quad (2)$$

c. Ozone was photolyzed to form O atoms in both the ground state $O(^3P)$ and the first excited state $O(^1D)$ (eq 3 and 4).

$$O_3 + h\nu \rightarrow O_2 + O(^1D) \quad (3)$$

$$O_3 + h\nu \rightarrow O_2 + O(^3P) \quad (4)$$

d. Most of the $O(^1D)$ became deactivated by collisions (eq 5), but some reacted with H_2O to form OH radicals (eq 6).

$$O(^1D) + M \rightarrow O(^3P) + M \quad (5)$$

$$O(^1D) + H_2O \rightarrow 2OH \quad (6)$$

e. Sulfur dioxide was oxidized mainly by reactions with OH for all relative humidities in the experiments (eq 7).

$$SO_2 + OH + M \rightarrow HSO_3 + M \quad (7)$$

f. For very low H_2O concentrations (below 2% relative humidity) SO_2 reactions with $O(^3P)$ began to have importance (eq 8) in nuclei formation even though the pre-

$$SO_2 + O + M \rightarrow SO_3 + M \quad (8)$$

ponderance of SO_2 oxidations appears to be via OH reaction. Also, HO_2 concentrations were so low under all experimental conditions that HO_2 was not important for SO_2 reactions (eq 9).

$$SO_2 + HO_2 \rightarrow SO_3 + OH \quad (9)$$

g. The HO_2 radical was generated by reaction of OH with O_3 (eq 10). However, conditions were always such

$$OH + O_3 \rightarrow HO_2 + O_2 \quad (10)$$

that the major gas-phase pathway for OH was reaction with SO_2 (eq 7).

h. The HO_2 radical termination (eq 11) is of no consequence in the analysis.

$$HO_2 + OH \rightarrow H_2O + O_2 \quad (11)$$

The experimental conditions that were maintained constant throughout the experiments are listed at the bottom of Table II. Under the flow conditions the time for irradiating the gaseous mixture of air, SO_2, and H_2O was 56 s in the system. The arrangement of the experimental reactor is shown schematically in Figure 2. Other pertinent details of the flow reactor system are the following:

a. The reactants and carrier gases were shown to be well mixed upstream of the radiation zone.

b. Flow through the radiation zone was laminar, allowing the calculation of ozone and free radical species in the system (see below).

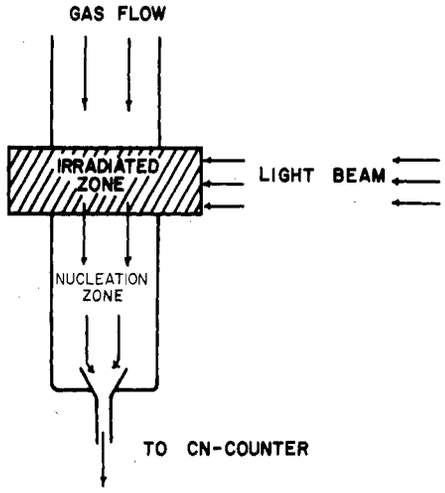

Figure 2. Schematic diagram of the experimental reactor illustrating the relationship of gas flow, region of irradiation, and region of nuclei formation.

c. Wall losses of SO_2 oxidation product were estimated by calculating a diffusion coefficient (assuming the product has a molecular weight of 98, which is equal to that of H_2SO_4 and nearly equal to that of $HSO_3 \cdot H_2O$) and by considering a wall collection efficiency of $\leq 10^{-2}$. The calculated loss is less than 0.2% with a diffusion coefficient of 0.10 $cm^2\ s^{-1}$ (see Fuller et al.[23] for a method of calculating binary gas-phase diffusivities).

Analysis of the chemical reactions and the associated rate coefficients (see Appendix) quickly reveals that ozone concentrations were far from the steady-state values. Some simple approximations were made for the geometry of the irradiated zone, permitting the development of an equation for ozone concentration that is linear in irradiation time. This permits calculation of similar linear relationships for $O(^1D)$ and OH concentrations. For all experiments the maximum concentrations of O_3 are calculated to have been $6.2 \times 10^8\ cm^{-3}$ by using eq A3 of the Appendix. Since the SO_2 concentration was constant throughout the system, the rate of reaction with OH varied linearly with time of irradiation within the restrictions of the approximations for the geometry of the irradiation zone. Nucleation was assumed to have occurred uniformly in the transit time (185 s) between the end of the irradiation zone and the entrance to the CN counter (see Figure 2). As will be seen later, the errors incurred by such approximations are of little importance to the qualitative conclusions and are small compared to the quantitative differences examined below.

For the purposes of the ensuing calculations and comparison to theory, we denote the product of the photooxidation of SO_2 by the symbol X. As mentioned above, the dominant pathway for SO_2 in all experimental conditions is assumed to be by way of reaction with OH radicals (eq 7). It has been generally assumed that X is H_2SO_4 and that reaction 7 represents the rate-limiting step in H_2SO_4 formation (see, for example, Hamill et al.[18] and Castleman et al.[11]). It will be shown later that, except for the lowest relative humidity conditions, H_2SO_4 is probably not the nucleating agent. The concentration of X at the point of emergence from the irradiated zone was calculated by integrating the linear expression for the rate of the SO_2 + OH reaction.

Table III lists calculated values of various quantities based upon the experimental conditions and the photochemical kinetics outlined in Table II and subject to the above assumptions. The first three columns all describe the water vapor concentrations and partial pressures

TABLE III: Concentrations of Important Species, Rates of Production of H_2SO_4 and Nuclei, and Rates of H_2SO_4 Binary Collisions[a]

1 rel humidity, %	2 p_{H_2O}, torr	3 $10^{-16} \cdot (H_2O)$, cm^{-3}	4a (OH), cm^{-3}	4b (OH), cm^{-3}	5 $10^{-3}Q$,[b] $cm^{-3}\ s^{-1}$	6 10^{-5}(X), cm^{-3}	7a[d] $10^8 \alpha_X$[c]	7b[e] $10^7 \alpha_X$[c]	8 (CN), cm^{-3}	9 J, $cm^{-3}\ s^{-1}$	10 Z_{AA}, $cm^{-3}\ s^{-1}$
1	0.238	0.772	262	258	4.18	2.34	1.87	2.18	109	0.59	9.36
5	1.19	3.86	1 310	1 080	21.0	11.7	9.40	11.9	174	0.94	234
10	2.38	7.72	2 620	1 800	41.8	23.4	18.7	21.8	927	5.0	936
25	5.94	19.3	6 540	3 000	105	58.6	46.8	54.4	10 900	59	5 800
50	11.9	38.5	13 000	3 860	208	117	93.6	109	29 000	160	23 200

[a] See text for full explanation. See bottom of Table II for other experimental conditions. [b] The production of rate of X. [c] The activity of X (see text). [d] Column a refers to $p^e_{H_2SO_4} = 3.6 \times 10^{-4}$ torr (ref 20). [e] Column b refers to $p^e_{H_2SO_4} = 3.1 \times 10^{-5}$ torr (ref 22).

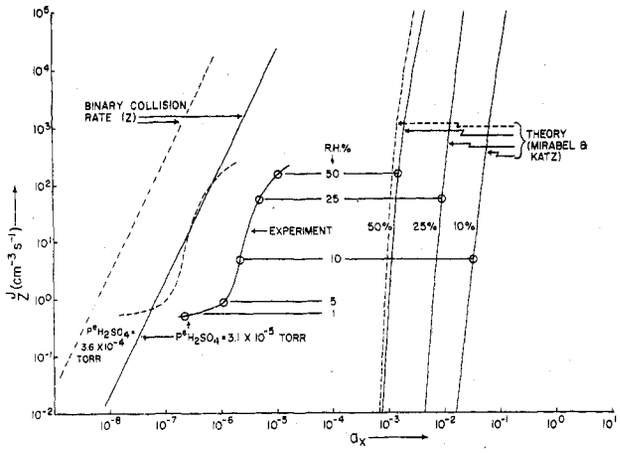

Figure 3. Nucleation and collision rates vs. H_2SO_4 or X activity. Solid curves correspond to $p^e_{H_2SO_4} = 3.1 \times 10^{-5}$ torr, and dashed curves correspond to $p^e_{H_2SO_4} = 3.6 \times 10^{-4}$ torr. See text for explanation of each curve.

(which are chosen to give convenient values of the relative humidities). Column 4a lists the calculated OH concentrations,[47] and column 5 gives the corresponding rate for the reaction SO_2 + OH, which is the production rate of X. Column 6 lists the calculated X concentration, and columns 7a and 7b are the ratios of the partial pressures of X to the equilibrium vapor pressure of pure H_2SO_4 liquid corresponding to the two different values discussed above. This quantity we denote by a_X in analogy to the activity.[48] Column 8 lists the observed concentration of condensation nuclei (CN) corresponding to the graph of the results of Leifer et al.[4] for the H_2O partial pressures. The listed CN concentrations were determined by correcting the measured concentrations for a constant background of about 100 cm^{-3} and for a dilution factor of about 6. Column 9 lists the calculated nucleation rates assuming the nuclei counted to have been formed in the 185-s transit time between the end of the irradiation zone and the inlet of the CN counter. Column 10 lists the rates of collisions of two X molecules (M_r = 98) according to the kinetic theory of gases. The formula for this is given below. It should be noted that the listed units of the quantities in columns 3, 4, 5, and 6 all have omitted the word "molecules", those of columns 8 and 9 have omitted the word "particles", and those in column 10 can be considered to have omitted the word "collisions".

For a mixture of gases the frequency of binary collisions of molecules of the same species, A, is

$$Z_{AA} = (\pi/(2)^{1/2})d^2\bar{c}C_A^2$$

where d = molecular diameter, here taken to be 5.5×10^{-8} cm, based on the molecular volume of pure liquid H_2SO_4 at 298 K, C_A = concentration of molecules A, (X), $\bar{c} = (8kT/\pi m)^{1/2}$, k = Boltzmann's constant, T = absolute temperature, and m = molecular mass of A (1.63×10^{-22} g for H_2SO_4).

It is to be emphasized that the nucleation rates, the X activities, and the binary collision rates for X listed in Table III are calculated quantities. The nucleation rates are closely related to the experimentally observed steady-state concentrations of the condensation nuclei. However, there is a rather long chain of theory that links the observed radiances, SO_2 concentrations, and H_2O frost points to X concentrations. It should be borne in mind that the attack of OH radical upon SO_2 may lead to species other than H_2SO_4 which can also create nuclei.

Figure 3 contains three representations of rate processes vs. activity (of X or H_2SO_4 with $p^e_{H_2SO_4} = 3.1 \times 10^{-5}$ torr), two of which are also listed in Table III. The curve designated as "experiment" is a plot of nucleation rate, J, calculated from the experimental observations shown in Figure 1 and listed in Table III. The line at the left is the rate of bimolecular collisions of X given by the equation for Z_{AA} above. It has a slope of 2, since Z varies with the square of the X concentration. The dashed curve and the line at the left of the figure are the similar experimental nucleation rates and bimolecular collision rates corresponding to $p^e_{H_2SO_4}$ equal to 3.6×10^{-4} torr. The right-hand curve is the theoretical nucleation rate–H_2SO_4 activity relationship for various relative humidities according to Mirabel and Katz.[16] These curves will be compared later in the paper with the experimental curve. The effect of hydrate formation in the theory (see Shugard et al.[17] and Shugard and Reiss[12]) was not considered by Mirabel and Katz[16] but is small relative to the differences depicted here.

IV. Discussion

A. Comparison of Nucleation Rates. Over the experimental range of relative humidities, the observed nucleation rates, which were reproducible to within about 15%, were much higher than theory would predict for given values of relative humidity and activity. However, this particular comparison is relatively meaningless, for, as Shugard and Reiss[12] have shown in a stochastic approach, very low nucleation rates would be theoretically subject to large fluctuations. The theoretically calculated nucleation rates would thus have no significance. We may note that the experimental conditions produced steady nucleation rates when unsteady rates are theoretically expected. Another comparison, which is obvious from Figure 3, shows that, to produce a given nucleation rate at a particular value of relative humidity, the experiments had activities considerably smaller than theory requires. These differences in activity are shown by the horizontal lines in Figure 3 indicated by relative humidity percent. The discrepancy between theoretical and experimental activities is more than two orders of magnitude at 50% relative humidity, and the discrepancy increases with decreasing relative humidity so that at 10% relative humidity it is more than four orders of magnitude. We therefore conclude that there is a substantial difference between the nucleation rates observed in our experiments and those which theory would predict if X were H_2SO_4. The observed rates are very much higher (by several orders of magnitude) and steadier than the theoretical rates.

B. Errors and Uncertainty. It is necessary to examine the assumptions and experimental observations for sources of errors and uncertainty. The oxidation rates of SO_2 depend mainly on several of the factors listed in the second column of Table II. The expression for this rate, Q, is

$$Q = 4\gamma \frac{j_1 j_3 k_6}{k_5} X_{O_2}(H_2O)t$$

where the j's and k's are given in Table II, (H_2O) is the concentration (in molecules cm^{-3}) of H_2O, t is the irradiation time for an average molecule in the experiment, X_{O_2} is the mole fraction of oxygen in air, and γ is a factor related to the geometry of the irradiated volume of the reactor. For the present purposes the value of γ is taken as unity. A derivation of a version of the above equation is given in the Appendix. We may arrive at an estimate of the uncertainty in Q by assuming the errors in each quantity to be uncorrelated and normally distributed on a logarithmic scale.[24] In this analysis the logarithm of the overall multiplicative fractional error is the square root of the sums of the squares of the logarithms of the individual

multiplicative fractional errors.[49] Random errors in (H_2O) and t arise from experimental measurements which are accurate to within a few percent, whereas the errors associated with the estimation of the j's and k's are considerably larger and dominate the overall error. The errors in the j's arise from uncertainties in the irradiance in the flow reactor and in the absorption cross sections. We crudely estimate the error in j_1 to be $\epsilon = 1.5$ on the basis of the discussion of O_2 cross sections by Hudson.[25] The absorption cross sections for O_3 are more accurately known than those for O_2 in the wavelength interval of interest in the experiment. We conservatively judge the error in j_3 to be about $\epsilon = 1.25$ on the basis of Hudson[25] and the report of the measurement of irradiances by Friend et al.[3] The reported experimental uncertainties in the k's and their references are the following: k_5, $\epsilon = 1.12$, ref 25; k_6, $\epsilon = 1.25$, ref 26; and k_7, $\epsilon = 1.3$, ref 27. The resulting overall error is $\epsilon = 1.8$ or $\langle Q \rangle / 1.8 \leq Q \leq 1.8 \langle Q \rangle$. This is our subjective estimate of the 95% confidence interval.

It was assumed that the nuclei detected in the experiments were formed uniformly in the region between the irradiated zone and the CN counter (Figure 2). The nucleation rates calculated on this basis are lower limits unless some type of induction is involved, which seems unlikely. Some rather cursory checks indicate that the observed CN concentrations vary roughly inversely with the flow rate through the reactor. Thus, it seems reasonable that nucleation was not duly nonuniform in the region designated as the nucleation zone in Figure 2, and nucleation may have been essentially uniform. The chemical mechanism presented in section D is in accord with the uniformity of nucleation throughout the nucleation zone.

The analysis of errors above also assumes that there was no loss of nuclei between the time of their creation in the nucleation zone and the time of their detection in the CN counter. Estimates of the loss rates of nuclei due to collisions with the walls were made on the basis of the chemical mechanism in section D of this paper. They show that for the experimental conditions such losses would range from a few percent for the lowest relative humidities (where the wall collection efficiency would be expected to be low) to no more than 40% for higher relative humidities. The value of 40% for wall losses corresponds to a wall collection efficiency of 100%. The effects of wall losses are not important to the principal qualitative aspects of the findings of this work. However, they are given further consideration in section D.

Aside from the above, a relative error of about ±15% can be associated with the nucleation rates based on the reproducibility of the CN-concentration measurements made a few months apart for the same conditions of flow rate, light intensity, and SO_2 and H_2O concentrations. Before the experiments the CN counter was calibrated at the factory against a Pollak counter, which is the standard instrument. This calibration, at the time it was made, is presumed to provide an accuracy of within ±15%. In view of the close reproducibility of the nuclei concentrations for duplicate experiments done a few months apart, we judge that an overall uncertainty in nucleation rate of ±30% would be a conservative estimate. However, this does not include any error due to lack of uniformity of production in the reactor. The question of the inherent ability of the CN counter to respond to the extremely small "particles" generated in our experiment is addressed in section C.

Returning to the comparison between theory and experiment (Figure 3), it is seen that (still assuming that X formation is determined by reaction 7) the uncertainty in Q is not nearly large enough to account for the differences in the curves. On the other hand the experimental J curve and the curve for Z may reasonably be related by the idea that nucleation is kinetically controlled.

Nucleation rates depend upon the activities of sulfuric acid, which are the ratios of $p_{H_2SO_4}$ to the equilibrium vapor pressure over the pure liquid at 25 °C. In their recent work Chu and Morrison[22] appear to provide a quite reliable value for the vapor pressure of sulfuric acid at 25 °C, as stated earlier. The effect of errors in this quantity can be seen by comparing the dashed curves in Figure 3 with the corresponding solid curves. This factor of more than 10 in $p^e_{H_2SO_4}$ is not sufficient to alter the qualitative discrepancies between the experimental and theoretical curves. It seems reasonable to expect that the error in the measured equilibrium vapor pressure is small compared to that which would alter the perceived qualitative difference between the theoretical and experimental nucleation rates.

C. H_2SO_4 or Free Radicals as Nucleating Agents. Guided by the numerical proximity of J and Z_{AA} (see Table III and Figure 3), we hypothesize that the observed steady state of nucleation proceeds along a kinetically controlled pathway, rather than along the thermodynamically controlled pathway envisioned in the theory of homogeneous nucleation. The experimental J curve is everywhere below the curve for Z for given a_X within the confidence limits discussed above. If it is assumed that the differences between the two arise because only a fraction of the binary collisions leads to nuclei precursors, then, by examining the ratio of column 9 to column 10 of Table III, one sees that this fraction is between 0.007 and 0.06. This analysis of Figure 3 and the ratio of column 9 to column 10 in Table III leads to the conclusion that approximately one in every 16–150 binary collisions of X results in a nucleus being formed. However, taking into account the uncertainty in nucleation rates, the acceptable range of the ratio of the rate of binary collisions to nucleation rate is 4–750. This can be contrasted to the requirement from the usual nucleation theory that for each nucleus formed there would be about 10^{10} or more binary collisions of H_2SO_4 molecules. It seems doubtful that the theory could be so far from correct in view of the recent experimental confirmation of binary homogeneous nucleation theory by Mirabel and Clavelin[19] for both HNO_3/H_2O and H_2SO_4/H_2O systems. Also, homogeneous nucleation of H_2O and other pure substances at high supersaturations seems to be well explained essentially by the same thermodynamic principle. (See Katz[30] for experimental evidence and Kiang et al.[31] for a discussion of the theory and problems related to it.) *We find it much more likely that the theory is simply not applicable because the substance responsible for nucleation is not H_2SO_4, but some other product of SO_2 oxidation such as the HSO_3 and/or HSO_5 radicals or possibly one or more of their hydrated forms.* The steep dependency of nucleation rate on water vapor concentration possibly implies participation of H_2O molecules beyond the role of furnishing OH radicals. In this regard the possibility of an enhanced SO_2 oxidation rate by hydrated OH radicals should not be ignored. An enhanced rate of the reaction

$$HO_2 + HO_2 \rightarrow H_2O_2 + O_2$$

caused by hydration of the HO_2 radical has been reported by Hamilton and Lii.[32]

The collision frequency, Z_{AA}, of X may be used as guidance in estimating the number of sulfur-bearing molecules that are required to make a nucleus. (Remember that a nucleus is that which will produce a droplet in the CN counter under conditions of 300% saturation in H_2O vapor.) We assume that X concentrations are rea-

sonable approximations of the concentrations of the real SO_2 oxidation products which form nuclei. The rate of collision of X molecules with clusters containing two of such molecules is roughly $Z_{AA}(X)^{-1}(CN)$, which is generally of the order of $(10^{-3}–10^{-2})Z_{AA}$ and would place the collision rate roughly at 10^{-1} of J over the experimental range. Therefore, though some nuclei may contain as many as three sulfur-bearing molecules, most are calculated to contain two.

The discussion in this section has shown that the observed nucleation cannot be explained reasonably by the theory of homogeneous heteromolecular nucleation. But rather it shows that the nucleation is most likely to be kinetically controlled and that almost all of the nuclei can contain no more than three sulfur-bearing entities. It is suggested that nuclei result from the combination of two free radicals to produce a single molecule containing two sulfur atoms.

This leads to an important question of the ability of the CN counter used in this experiment to detect such small "particles" as we apparently have seen. It is clear that the nuclei were photochemically created from SO_2 and that their rates of formation were kinetically controlled. As indicated above, it is likely that the nuclei contain two or fewer sulfur atoms per nucleus. Thus, we conclude that the entities detected by the CN counter consisted of one or two molecules of a compound or compounds containing one or two sulfur atoms plus associated H_2O molecules. Liu and Kim[33] have found that a General Electric CN counter similar in operation to the one used in the experiments of Leifer et al.[4] was quite inefficient for detecting NaCl particles with diameters less than 10^{-2} μm. They caution against indiscriminate interpretation of CN-counter results for such ultrafine aerosol particles. However, the argument presented here shows that the counter responds to "particles" which are of molecular sizes. We wish to suggest that the sulfur-compound/H_2O aerosol found in the experiments of Leifer et al.[4] was of such a different nature from the NaCl aerosols studied by Kim and Liu[33] that one should not expect these acidic, sulfur nuclei to have detection efficiency–size relationships comparable to NaCl.

D. Shape of the Experimental Nucleation Rate Curve and a Mechanism of Nucleation. There are three striking features of the experimental curve of J shown in Figure 3: the sharp change in slope around 2% relative humidity, the steepness of the slope for relative humidity from 2% up to about 25%, and the decrease of slope at higher values of relative humidity. It is the general practice in chemical kinetics to set forth a mechanism which explains the observed rate data. We maintain this practice here, while recognizing that the approach may be somewhat simplistic because of the relatively complicated nature of the experiment wherein H_2O was involved in furnishing the hydroxyl radical and apparently in forming compounds with the oxidation products of SO_2. In setting forth the model we were aware of the work of Hamilton and Lii,[32] who studied the recombination reactions of HO_2 in the presence of H_2O in one set of experiments and NH_3 in another set. In both cases it was found that the presence of the added gases enhanced the radical recombination rates. The mechanism which Hamilton and Lii[32] suggest to explain their observations involved equilibrium steps to form addition compounds such as $HO_2{\cdot}H_2O$ and $HO_2{\cdot}NH_3$. Then, for each system there were found three recombination reactions of the type:

$$\mathrm{R} + \mathrm{R} \rightarrow \text{products} \qquad \text{(i)}$$

$$\mathrm{R{\cdot}X} + \mathrm{R} \rightarrow \text{products} \qquad \text{(ii)}$$

$$\mathrm{R{\cdot}X} + \mathrm{R{\cdot}X} \rightarrow \text{products} \qquad \text{(iii)}$$

We propose the following mechanism to explain nucleation in the SO_2, H_2O, O_2–N_2 system in the presence of radiation of suitable wavelengths:

$$SO_2 + OH + M \rightarrow HSO_3 + M \qquad k_7 \qquad (7)$$

$$SO_2 + OH = [HSO_3]^* \qquad K_{12} \qquad (12)$$

$$[HSO_3]^* + M \rightarrow HSO_3 + M \qquad k_{13} \qquad (13)$$

$$[HSO_3]^* + H_2O = [HSO_3{\cdot}H_2O]^* \qquad K_{14} \qquad (14)$$

$$[HSO_3{\cdot}H_2O]^* + M \rightarrow HSO_3{\cdot}H_2O + M \qquad k_{15} \qquad (15)$$

$$HSO_3 + HSO_3 \rightarrow N_{00} \qquad k_{16}\langle 00\rangle \qquad (16\langle 00\rangle)$$

$$HSO_3 + HSO_3{\cdot}H_2O \rightarrow N_{01} \qquad k_{16}\langle 01\rangle \qquad (16\langle 01\rangle)$$

$$HSO_3{\cdot}H_2O + HSO_3{\cdot}H_2O \rightarrow N_{11} \qquad k_{16}\langle 11\rangle \qquad (16\langle 11\rangle)$$

$$HSO_3{\cdot}iH_2O + HSO_3{\cdot}jH_2O \rightarrow N_{ij} \qquad k_{16}\langle ij\rangle \qquad (16\langle ij\rangle)$$

$$HSO_3{\cdot}iH_2O + O_2 + M \rightarrow HSO_5{\cdot}iH_2O + M \qquad k_{17}\langle i\rangle \qquad (17\langle i\rangle)$$

$$HSO_3{\cdot}iH_2O + HSO_5{\cdot}jH_2O \rightarrow NN_{ij} \qquad k_{18}\langle ij\rangle \qquad (18\langle ij\rangle)$$

$$HSO_5{\cdot}iH_2O + HSO_5{\cdot}jH_2O \rightarrow NNN_{ij} \qquad k_{19}\langle ij\rangle \qquad (19\langle ij\rangle)$$

$$SO_2 + O + M \rightarrow SO_3 + M \qquad k_8 \qquad (8)$$

$$SO_3 + H_2O + M \rightarrow SO_3{\cdot}H_2O + M \qquad k_{20} \qquad (20)$$

$$SO_3{\cdot}H_2O \rightarrow N_1 \qquad k_{N1} \qquad (N1)$$

The symbols containing N's denote a nucleus, and the subscripts indicate the number of H_2O molecules in the nucleus deriving from a particular radical. Thus the term NN_{ij} indicates a nucleus formed from the association of $HSO_3{\cdot}iH_2O$ with $HSO_5{\cdot}jH_2O$ and having i plus j H_2O molecules. Examination of the list should make the designation scheme clear. It should be noted that N_1 denotes a nucleus resulting from a single molecule of $SO_3{\cdot}H_2O$ via a first-order reaction (N1).

The composite of the presumed fast equilibrium reaction (reaction 12) and the rate-limiting deactivation of the high-energy intermediate state HSO_3^* (reaction 13) is reaction 7. We have chosen this form to present the formation of HSO_3 in order to show the plausibility of forming $HSO_3{\cdot}H_2O$ via reactions 14 and 15 in a parallel pathway to HSO_3 formation. The composite of reactions 12, 14, and 15 is

$$SO_2 + OH + H_2O + M \rightarrow HSO_3{\cdot}H_2O + M \qquad (21)$$

whose rate may be written

$$R_{21} = k_{21}(SO_2)(OH)(H_2O)$$

so that we may compare k_{21} to k_7 by using the relationship

$$k_{21} = bk_7 \qquad (22)$$

where b is a dimensionless constant.

We emphasize that eq 21 does not represent an elementary reaction and, further, that the constant k_{21} has in it a factor of (M). We think that eq 12, 14, and 15 are reasonable to propose as elementary reactions for the model mechanism. As will be seen, in order for the mechanism to provide a dependency of nucleation rate upon H_2O concentration similar to the observed dependency, it is necessary to postulate the production of $HSO_3{\cdot}H_2O$ in a path parallel to HSO_3 production rather than in a serial path following the production of HSO_3.

For computational purposes the model mechanism can be represented as beginning with the two reactions

$$SO_2 + OH + M \rightarrow HSO_3 + M \quad (7)$$

$$SO_2 + OH + H_2O \rightarrow HSO_3{\cdot}H_2O \quad (7')$$

the second of which has an effective third-order rate coefficient

$$k_{7'} = bk_7 \quad (7'')$$

Nuclei production in the model for ≥5% relative humidity proceeds from the various radical–radical association reactions among HSO_3, $HSO_3{\cdot}H_2O$, and their reaction products with O_2, namely, HSO_5 and $HSO_5{\cdot}H_2O$. These processes are represented by reactions 16⟨00⟩ through 19⟨ij⟩ in the model mechanism. We note that we cannot now distinguish among the various association reactions of HSO_3 and HSO_5 and their hydrates. That is to say, if reactions 17⟨i⟩ are rapid enough (and they are expected to be; see Davis et al.[34]), HSO_5 could be the principal radical involved in nucleus formation by way of reactions 19⟨ij⟩. There is, of course, the possibility of HSO_3/HSO_5 associations (reactions 18⟨ij⟩) which also cannot be distinguished from one another. Thus in order to avoid unnecessary complexity we denote by the symbol R_i any sulfur radical having i waters of hydration. We may now represent the proposed model mechanism as the following:

$$SO_2 + OH + M \rightarrow HSO_3 + M \quad k_7 \quad (7)$$

$$SO_2 + OH + H_2O \rightarrow HSO_3{\cdot}H_2O \quad k_{7'} \quad (7')$$

$$SO_2 + O + M \rightarrow SO_3 + M \quad k_8 \quad (8)$$

$$HSO_3{\cdot}iH_2O + O_2 + M \rightarrow HSO_5{\cdot}iH_2O + M \quad k_{17\langle i\rangle} \quad (17\langle i\rangle)$$

$$R_i + R_j \rightarrow N_{ij} \quad K_{Nij} \quad (Nij)$$

$$SO_3 + H_2O + M \rightarrow SO_3{\cdot}H_2O + M \quad k_{20} \quad (20)$$

$$SO_3{\cdot}H_2O \rightarrow N_1 \quad k_{N1} \quad (N1)$$

A further simplification which we make here is to assume that $i,j = 0,1$; i.e., no radical hydrates having more than one H_2O molecule are considered. This may not be the case, but to permit higher hydrates would introduce more parameters into the problem than we feel are justified.

Reactions 8, 20, and N1 account for the formation of nuclei for ≤1% relative humidity. Reactions 7, 7′, 17, and Nij account for nucleation for >5% relative humidity. The region between 1 and 5% relative humidity is transitional where both mechanisms contribute significantly to nucleation.

The proposed mechanism permits calculation of the concentrations of the important reactive species generated in the irradiated zone. The OH concentration is a linear function of the distance along this zone (or of irradiation time) and of the O-atom concentration, which is uniform throughout the zone (see Appendix). The OH concentration, taking into account reaction 7′, was calculated from eq A5 and is listed in column 4b of Table III for various values of (H_2O). The initial conditions for the reaction species in the nucleation zone are derived from conditions in the irradiation zone with $t = \tau_r$, the residence time of the air in the irradiation zone. The nucleation reactions are presumed to be slow enough so as not to remove significant amounts of the reactive species generated. An estimate of the rate coefficient of reaction 13 has been given by Castleman et al.[11] to be 9×10^{-13} cm^3 molecule^{-1} s^{-1}, which is large enough so that at even the lowest H_2O concentrations essentially all of the SO_3 produced in the irradiation zone becomes hydrated there. As a result, the concentration of $SO_3{\cdot}H_2O$ at the boundary of the nucleation zone is

$$(SO_3{\cdot}H_2O)_0 = (2j_1k_8,/k_2)(SO_2)\tau_r \quad (23)$$

The concentrations of R_i (R_0 and R_1) at the boundary of the nucleation zone are found by integrating the rate expressions of eq 24 and 25, which are valid over the irradiation zone if radical–radical association reactions proceed at negligible rates. The OH concentration, as a function of time in the irradiation zone, is given in the Appendix (eq A5). The resulting concentration expressions are given in eq 26 and 27, where $a = 2j_1j_3(O_2)k_6/k_5 = 1.28$

$$d(R_0)/dt = k_7(SO_2)(OH)(M) \quad (24)$$

$$d(R_1)/dt = k_{7'}(SO_2)(OH)(H_2O) \quad (25)$$

$$(R_0)_0 = \frac{a(H_2O)\tau_r^2}{[(M) + b(H_2O)]} \quad (26)$$

$$(R_1)_0 = \frac{ab(H_2O)^2\tau_r^2}{[(M) + b(H_2O)](M)} \quad (27)$$

$\times 10^5$ molecules cm^{-3} s^{-2} for all conditions of the experiments (see Table II). The assumption that nucleation is not rapid enough to deplete (R_i) and $SO_3{\cdot}H_2O$ in the nucleation zone makes the relationships 23, 26, and 27 valid for the entire nucleation zone. The nucleation rate is then

$$J = k_{N00}(R_0)^2 + k_{N01}(R_0)(R_1) + k_{N11}(R_1)^2 + k_{N1}(SO_3{\cdot}H_2O) \quad (28)$$

Using eq 24, 26, and 27, one can express the nucleation rate as a function of water vapor concentration:

$$J = \frac{[A(H_2O)^4 + B(H_2O)^3 + C(H_2O)^2]}{[(M) + b(H_2O)]^2} + D \quad (29)$$

where

$$A = \frac{a^2b^2\tau_r^4}{(M)^2}k_{N11}$$

$$B = \frac{a^2b\tau_r^4}{(M)}k_{N01}$$

$$C = a^2\tau_r^4k_{N00}$$

$$D = \frac{2j_1k_8}{k_2}(SO_2)\tau_rk_{N1}$$

A curve-fitting procedure was developed by using a least-squares criterion, plus other criteria linked to the shape of a curve through the experimental data shown in Figure 1. Specifically, we tried to capture the qualities of steep slope between 5 and 25% relative humidity and of curving to shallower slopes for relative humidity greater than 25%. This is not an entirely objective procedure, so that the results given below should be taken as indicative of a plausible set of rate coefficients which fit the data as closely as can be done within the limited scope of the model. Other qualifying remarks are given below based upon the computer-assisted explorations of model curves to fit the data. A plot of the "best fit" model J vs. (H_2O) is shown in Figure 4 along with the data; the values of the various rate coefficients in the model are $k_{N00} = 6 \times 10^{-14}$ cm^3 molecule^{-1} s^{-1}, $k_{N01} = 3 \times 10^{-12}$ cm^3 molecule^{-1} s^{-1}, $k_{N11} \leq 1 \times 10^{-20}$ cm^3 molecule^{-1} s^{-1}, $k_{N1} = 1.3 \times 10^{-4}$ s^{-1}, and $b = 170$. Therefore, $k_{22} = 170k_7 = 3.9 \times 10^{-30}$ cm^6 molecule^{-2} s^{-1}. These general remarks can be made about the rate constants in the model:

a. The quantity which appears to affect the fitting process the most, and is therefore the "best determined",

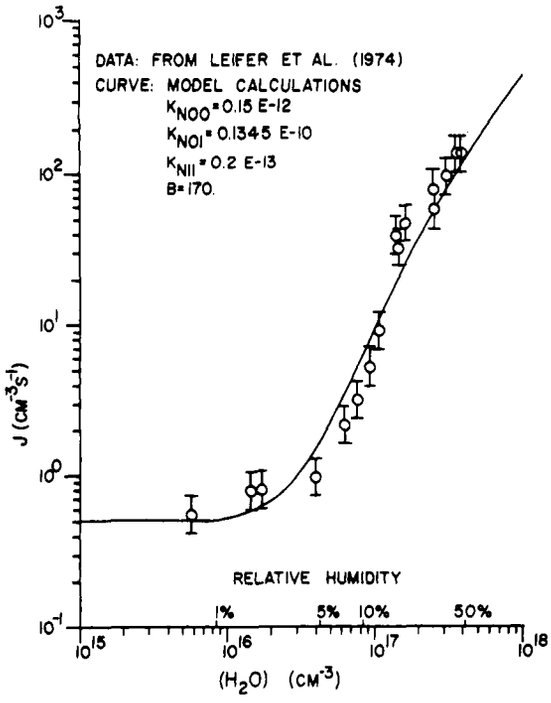

Figure 4. Nucleation rates vs. H_2O concentration. The curve represents the results of model calculations (see text). The points are the data from Leifer et al.[4] The error bars pertain to estimates of uncertainty in the measurement of CN concentrations.

is k_{N01} for which acceptable values were not found outside the range of ±20% of the value given above.

b. The next most important quantity is b which for values between 170 and 200 produced acceptable fittings.

c. The value of k_{N00} is not sensitively determined by the curve-fitting procedure, and that given above should be considered as indicating the order of magnitude only.

d. The quantity k_{N11} can only be said to be substantially smaller than k_{N01} and k_{N00}.

e. The value of k_{N1} was chosen to give a limiting value (as relative humidity → 0) for J which would reasonably agree with the experimental results for relative humidities less than 5%. It appears that values within ±30% of the chosen value would provide such reasonable agreement.

We judge that within these ranges the rate coefficients provide a fit of the model (eq 29) within our own, somewhat subjective criteria. These ranges are not to be considered as estimates of uncertainties in the rate coefficients since there is no assurance that the model is correct in detail. In fact, perusal of Figure 4 shows that the model (eq 29) fails to depict all of the significant features of the data, since the equation does not fall within the estimated error limits along certain portions of the data. It is evident that the model does not adequately represent all of the processes which occur. Nonetheless the major features of the J vs. (H_2O) dependence are seen to be captured by the model. In the model framework nucleation rates, J, for the higher range of water vapor concentrations (values of relative humidity from 5 to 50%) are dominated by the term in $(H_2O)^3$ in the numerator of eq 29, which corresponds to the term in $(R_0)(R_1)$ in eq 28. Over this range of (H_2O) the creation of condensation nuclei occurs via the reactions of hydrated with unhydrated free radicals (such as reactions 16⟨01⟩, 18⟨01⟩, and 19⟨01⟩). The diminishment in slope toward the higher end of the range is controlled by the denominator in eq 29 and reflects the increased production of hydrated free radicals relative to the production of unhydrated species. (Compare eq 26 and 27 in the limit of $b(H_2O) \gg (M)$.) The curve-fitted value of k_{N11} is so small that reactions among hydrated species in the model contribute negligibly over the entire experimental range of (H_2O).

The reactions of hydrated SO_3 dominate the model nucleation rates for ≤1% relative humidity, which accounts for the nondependence of J on (H_2O) for that region. This is shown by the expression for the term D in eq 29 or by eq 23. The value of K_{N00} is small enough that reactions among unhydrated free radicals (R_0 with R_0) are of secondary importance within the model. More important are the reactions of $SO_3 \cdot H_2O$ at low concentrations of H_2O and of R_0 and R_1 at higher H_2O concentrations. Thus, the region from 1 to 5% relative humidity marks a transition where both $SO_3 \cdot H_2O$ and $R_0 + R_1$ reactions contribute significantly to the creation of nuclei and reactions of $R_0 + R_0$ are quite minor. The value of the rate coefficient which dominates the OH-induced nucleation process ($k_{N01} = 0.3 \times 10^{-11}$ cm^3 $molecule^{-1}$ s^{-1}) is not unreasonable for a radical–radical reaction; that is, it is within a factor of 4 of the reported rate coefficients[28] for the reactions HS + HS → H_2S + S (1.2×10^{-11} cm^3 $molecule^{-1}$ s^{-1}) and Cl + ClOO → 2ClO (1.1×10^{-11} cm^3 $molecule^{-1}$ s^{-1}), while it is yet smaller than the reported values for the reactions HO + HO_2 → H_2O + O_2 (3×10^{-11} cm^3 $molecule^{-1}$ s^{-1}), HO_2 + Cl → HCl + O_2 (3×10^{-11} cm^3 $molecule^{-1}$ s^{-1}), and Cl + ClOO → Cl_2 + O_2 (1.6×10^{-10} cm^3 $molecule^{-1}$ s^{-1}).

The nucleation model we have proposed contains several simplifying aspects. For example, it does not distinguish between HSO_3 and HSO_5 radicals or between their respective hydrates. Furthermore, the formation and reactions of higher hydrated species ($i \geq 2$) are ignored. All of these factors are of potential importance in understanding the actual mechanism of nucleation and may have a bearing on the systematic differences between the model curve and the experimental data, as shown in Figure 4. However, as indicated previously, we believe that the imposed simplifications prevent the proliferation of model parameters which would not, in any case, be well determined. During the course of the investigation we tried, in the manner of Hamilton and Lii,[32] to use a model in which the hydrated radicals formed serially from R_0 and were in equilibrium via

$$R_0 + H_2O \rightleftharpoons R_1 \qquad (30)$$

However, the resulting expression for J had a dependency on (H_2O) which was not sufficiently steep for relative humidities greater than 5%. For this reason, reactions via eq 30 were replaced with the somewhat more complicated set of reactions in the model. We feel that this model provides insight into the photochemical processes of nuclei formation in the SO_2, O_2, H_2O system, particularly concerning the role of hydrated free radicals.

A possible product of HSO_3 recombinations is dithionic acid, $H_2S_2O_6$, and a possible product of the reaction of HSO_3 and HSO_5 is peroxodisulfuric acid, $H_2S_2O_8$, which may also result from HSO_5 recombinations (with O_2 being a second product). In light of the mechanism discussed above it would appear that the molecular species (which are, in effect, condensation nuclei in the experiment) are at least single hydrates of SO_3 (for <5% relative humidity) and $H_2S_2O_6$ and/or $H_2S_2O_8$ (≥2% relative humidity), with higher hydrates possible. This is commensurate with the discussion of section C in that the substance X, the product of SO_2 + OH reactions, is either or both of HSO_3 and HSO_5 and their hydrates. The creation of nuclei is controlled by reactions among those radicals, and the products of such reactions, hydrates of $H_2S_2O_6$ and $H_2S_2O_8$, are likely to be the nuclei. That is, a single hydrated molecule of $H_2S_2O_6$ or $H_2S_2O_8$ is sufficient to produce a droplet in a conden-

sation nuclei counter operated at 300% relative humidity. It is of interest to note that the ammonium salt of $H_2S_2O_8$ has been detected in stratospheric aerosol collections.[35] It is possible that a reaction sequence similar to the mechanism proposed here with reactions 18 and/or 19 could account for those stratospheric aerosols.

The single molecules produced by the radical recombinations suggested above would be susceptible to losses by wall collisions in the reactor as mentioned in section C. If the properties of these molecules are similar to H_2SO_4, then their removal efficiency would be expected to be low (of the order of a few percent or less) for the lowest relative humidity and would be expected to increase as relative humidity increases. We have estimated that the maximum wall loss, corresponding to 100% removal efficiency, would remove 40% of the molecules formed in the nucleation zone of the reactor before reaching the detector. Since we do not know the actual wall loss rate as a function of H_2O concentration, its effect could not be included explicitly in the considerations of the mechanism and the estimation of the reaction rate coefficients. It can be seen in reference to Figure 4 that the effect of correcting for a H_2O-concentration-dependence loss would be to steepen the model curve by increasing the nucleation rates for the higher relative humidities. This would have the tendency to make the model mechanism curve in Figure 4 more nearly parallel with the implied experimental curve. The net effect of considering corrections for possible wall losses of nuclei in the reactor would be to change the derived rate coefficients by a factor of about 20% or less and to increase the goodness of fit of the model curve with the observed nucleation rates. The principal qualitative aspects of the proposed mechanism of nuclei formation remain unaltered by the consideration of corrections for loss of nuclei by wall collision.

The reactions that form the two sulfur atom–molecules discussed above would account for the formation of nuclei at relative humidities greater than 5% in the experiments. As mentioned above, the model suggests that nucleation for relative humidity less than 1% is primarily due to $SO_3{\cdot}H_2O$ (reactions 20 and N1). It is instructive to examine the relative rates of production of SO_3 and R (equal to $R_0 + R_1$) for various concentrations of water vapor. The ratio of these rates, derived in the Appendix (eq A.9), is expressed as

$$\Gamma = E(H_2O)^{-1}[(M) + b(H_2O)] \quad (31)$$

where E is a constant under the experimental conditions. For $(H_2O) = 7.7 \times 10^{15}$ cm^{-3} (1% relative humidity) that ratio has the value of 0.03. Thus we arrive at an interesting model result that 3% of the SO_2 oxidation reactions give rise to more than 90% of the nuclei formed at a relative humidity of 1%. In fact the model indicates that the O-atom reaction (eq 8) is relatively more powerful in nucleation than the OH reactions (eq 7 and 7′) over the entire experimental range of (H_2O). However, at 50% relative humidity the O-atom reaction creates 0.3% of the nuclei and is responsible for 0.2% of the SO_2 oxidations. This reflects the effectiveness of first-order kinetic processes (eq N1) within the model relative to second-order processes (eq Nij). It seems reasonable to associate the first-order nucleation reaction (eq N1) with the chemical transformation

$$SO_3{\cdot}H_2O \rightarrow H_2SO_4 \quad (32)$$

A recent study by Holland and Castleman[36] examined the stability of $SO_3{\cdot}H_2O$ relative to H_2SO_4 by using an approximate molecular orbital calculation. The complex was found to be stable with respect to formation from SO_3 and H_2O and relatively less stable than H_2SO_4, but with a 3.3 kcal/mol barrier to rearrangement to H_2SO_4. The structure of the $SO_3{\cdot}H_2O$ complex with minimum energy has a pair of electrons from the H_2O oxygen directed toward the sulfur atom of SO_3. Although such calculations may not be reliable in detail, the relative stabilities should be reasonably represented.[37] Therefore, it may be that the first-order nucleation process is identical with the process of isomerization (rearrangement) of the complex $SO_3{\cdot}H_2O$ to H_2SO_4. According to the theory of activated complexes, k_{N1} would characterize the rate of conversion to H_2SO_4 of $SO_3{\cdot}H_2O$ molecules that have an energy sufficient to pass over the peak of the barrier between the relatively stable $SO_3{\cdot}H_2O$ and H_2SO_4. It would thus appear that at the lowest relative humidity values attained in our experiments it is possible that gaseous H_2SO_4 may indeed be important in nucleation. If so, however, the condensation nucleus is a single molecule (aside from possible waters of hydration). This situation would still be vastly different from that described by the theory of heteromolecular homogeneous nucleation of H_2SO_4 and H_2O.

In arriving at the decision to propose eq 8, 20, and N1 as a mechanism to explain nucleation at low relative humidity values, we considered several second-order reactions as possible candidates for the nucleation step (eq 33–35).

$$SO_3{\cdot}H_2O + SO_3{\cdot}H_2O \rightarrow N \quad (33)$$

$$SO_3{\cdot}H_2O + H_2O \rightarrow N \quad (34)$$

$$SO_3{\cdot}H_2O + HSO_3 \rightarrow N \quad (35)$$

Each of these reactions gave at least a first-power dependency of J on (H_2O) and so could not be fit for relative humidity less than 5%. Furthermore, in trying to find a numerical fit, we found that the rate coefficients for such reactions would have to be larger than "gas-kinetic" by about an order of magnitude. Therefore, although these reactions may actually occur to some extent, and they could have some significance in the region near 5% relative humidity, they are probably unimportant for relative humidity values below a few percent. Faced with the virtual impossibility of explaining the flat portion of the nucleation curve by a second-order reaction, we concluded that a first-order nucleation step would be adequate and could be a close representation of the actual mechanism. This conclusion is commensurate with the idea that a nucleus consists of a single stable sulfur molecule and associated water molecules. Though our model cannot account for all of the observed features of the nucleation rate dependency on (H_2O), it provides general support to the notion that nucleation by SO_2 photooxidation is kinetically controlled and that the mechanism is a reasonable approximation of the important chemical processes involved.

E. Unimportance of $SO_2 + h\nu \rightarrow SO_2^*$. Friend et al.[3] showed that the quantum yield for the products of the process

$$SO_2 + h\nu(240\text{–}340\text{ nm}) \rightarrow SO_2^* \xrightarrow{O_2} \text{products}$$

is less than 10^{-9} and is therefore of no consequence in producing nuclei either in the reactor or in the atmosphere. The particular evidence for this result was the comparison of CN concentrations caused by irradiation of air and SO_2, first in the wavelength region where only SO_2 would be excited and next in the region where O atoms would be formed and SO_2 would be excited. In the first case no nuclei were detected so that $(CN) \leq 140$ cm^{-3}, whereas in the second case (CN) was equal to 3×10^5 cm^{-3}. For these experiments, the water vapor concentration was very low (<0.1% relative humidity) so that the O-atom oxidation

mechanism (reaction 8) used to calculate sulfate production rates was valid. The experimental evidence, as analyzed by Friend et al.,[3] shows that, with respect to nuclei production, free radical oxidation of SO_2 greatly dominated over any process which involves the photoexcitation of SO_2 in the wavelength region of 240–340 nm.

The quantitative aspects of the analysis of Friend et al.[3] remain essentially unchanged by any of the considerations put forth in the present work except that the rate coefficient for reaction 2 is now taken to be nearly a factor of 2 higher. Thus the upper limit of the quantum yield for SO_2 photolysis (to yield products) in the experimental system should be approximately 2×10^{-9}.

This quantum yield is in apparent conflict with the laboratory findings of others such as Cox,[37] Allen et al.,[38] and most recently Marvin and Reiss,[8] who studied systems in which chemical reactions of SO_2 with SO_2* were thought to be probable. Under those conditions the quantum yield of SO_2 photolysis was found to be of order of 10^{-4} (see ref 37, 38, and 8). The conditions of the experiments discussed in this paper[3,4] provided generally lower SO_2 concentrations and shorter irradiation times than the above referenced experiments.

F. Comparison with Other SO_2 Nucleation Experiments. There have been several experiments reported in which SO_2 was photooxidized to form condensation nuclei. Most of them have been briefly summarized in Appendix 2 of Kasahara and Takahashi[6] and will not be repeated here, since it is our main purpose to discuss the chemical processes important in nucleation and not to compare and criticize experiments. Therefore, we will mention only those studies in which attempts were made to propose a chemical mechanism or which we feel have a readily perceived direct relevance to the mechanism proposed in this paper.

The study of Marvin and Reiss[8] using a thermal gradient diffusion cloud chamber was a carefully controlled set of measurements which were interpreted as proceeding according to the sequence:

$$SO_2 + h\nu \rightarrow SO_2^* \quad (36)$$

$$SO_2^* + SO_2 \rightarrow SO_3 + SO \quad (37)$$

$$SO_3 + H_2O \rightarrow H_2SO_4 \xrightarrow[H_2O]{} \text{nucleus} \quad (38)$$

There was little or no possibility for O-atom or OH radical formation. The $SO_3 \cdot H_2O$, H_2SO_4, and hydrated H_2SO_4 which were formed may indeed have been single-molecule condensation nuclei in a CN counter such as used in Friend et al.[3] However, under conditions in the thermal diffusion cloud chamber the growth to large droplets appears to have been controlled by the binary homogeneous nucleation mechanism.[8] It should be noted that Marvin and Reiss suggest that dependency of the rate coefficient of the reaction of SO_2* with SO_2 upon (H_2O) is due possibly to the formation of SO_2 hydrates. It is difficult to compare quantitatively the results of Marvin and Reiss' work with those of Friend et al.[3] and Leifer et al.[4]

Cox[39] performed experiments similar to those of Friend et al.[3] using a slow flow reactor and a CN counter. When radiation of 185-nm wavelength was used, the observed nucleation in the absence of O_2 was attributed to the sequence

$$SO_2 + h\nu \rightarrow SO + O \quad (39)$$

$$SO_2 + O + M \rightarrow SO_3 + M \quad (40)$$

$$SO_3 + H_2O \xrightarrow[m]{} H_2SO_4 \xrightarrow[H_2O]{} \text{nuclei} \quad (41)$$

When radiation with wavelengths greater than 290 nm were used, nucleation was observed in the absence of O_2, which appears to be in contradiction to the findings of Friend et al.[3] When O_2 was present and $\lambda \geq 290$ nm, Cox[39] found (CN) to be 10–100 times higher than with no O_2 present. The formation of nuclei in the absence of O_2 was attributed to reactions 42 and 43. No detailed mechanism

$$SO_2^* + SO_2 \rightarrow SO_3 + SO \quad (42)$$

$$SO_3 + H_2O \rightarrow H_2SO_4 \xrightarrow[H_2O]{} \text{nuclei} \quad (43)$$

was proposed to account for nucleation with O_2 present. Cox[39] presumed that H_2SO_4 was created following photoexcitation of SO_2. Smith, DePena, and Heicklen[40] performed an experiment using a static reaction vessel with O_2 present and with radiation of wavelengths greater than 300 nm. They also found nucleation to occur. However, fairly scattered results made precise quantitative interpretation difficult. They showed that their results were similar to those obtained by Cox[39] and offered the suggestion that the observed nucleation could be explained by the mechanism:

$$SO_2^* + O_2 \rightarrow SO_4 \quad (44)$$

$$SO_4 + SO_2 \rightarrow 2SO_3 \quad (45)$$

$$SO_3 + H_2O \rightarrow H_2SO_4 \quad (46)$$

$$qSO_4 \rightarrow (SO_4)_q \quad [= \text{nucleus}] \quad (47)$$

The first two steps listed here were suggested by Leighton[41] as a route to H_2SO_4 from SO_2 photoexcitation. Smith et al.[40] proposed that the clustering of an undetermined number, q, of SO_4 molecules represents the nucleation process and the resultant entity $(SO_4)_q$ is the center for condensation of H_2SO_4 (and presumably H_2O) molecules.

It is difficult to make direct comparisons between the experiments of Friend et al.[3] and Leifer et al.[4] on the one hand and those of Cox[39] and Smith et al.[40] on the other hand because of differences in SO_2 concentrations, light intensities, and irradiation times. The longer irradiation times of Cox[39] and Smith et al.[40] could have been accompanied by significant wall losses of aerosol precursors and of aerosol particles, and their experiments could have been subject to the effects of contaminants to which static experiments in nucleation are especially vulnerable. However, the chemical mechanism proposed by Smith et al.[41] is qualitatively different from that proposed in this paper, and it arises from qualitative differences in observations. Friend et al.[3] could observe no increase in (CN) over background for wavelengths greater than 250 nm and arrived at the conclusion that the quantum efficiency for $SO_2 + h\nu \rightarrow SO_2^* \rightarrow$ products was not more than about 10^{-9}. Cox's experiments using nearly the same radiation intensities, about 5 times the SO_2 concentrations, and about 2.5 times the irradiation time produced concentrations of CN of about 10^3 times the background CN concentrations of Friend et al.[3] We are not sure of the reason for such disparate observations. However, we suspect that contamination effects, such as those shown experimentally by Friend et al.[3] to occur when sources of trace organic gases such as plastic tubing or stopcock grease are present, could have caused the nuclei observed by Cox[39] and by Smith et al.[40] Also, we note that reproducibility of the experiments by Leifer et al.[4] was quite good (within ±15% of measured (CN)), whereas that illustrated by Cox[39] (see his figure 3) shows deviations from one time to another up to a factor of 3. The experiments of Smith et al.[40] showed considerably larger variability in the maximum number concentrations of nuclei produced.

The next comparison made here is with the experiments of Bricard et al.[2] who showed that the presence of NO_2 enhanced nuclei formation when SO_2 and air mixtures were irradiated ($\lambda > 300$ nm), though like Cox[39] and Smith et al.[40] (and probably for similar reasons) they also observed nucleation without NO_2 present in that wavelength region. Nonetheless, the effect of NO_2 is in qualitative agreement with the mechanism proposed in this paper since it is a source of O atoms under the conditions of irradiation.

Recent work by McMurry and Friedlander[42] involved experiments in the formation of nuclei by irradiation of air containing ambient aerosol and added amounts of SO_2, NO, NO_2, and propylene. The rates of formation of new nuclei in the presence of aerosol were explained as being consistent with an activationless kinetic process, as opposed to homogeneous nucleation with a free energy barrier ($=\Delta G^*$) discussed at the beginning of this paper. The gas mixtures used by McMurry and Friedlander[42] are known to produce O atoms and OH radicals. Thus the oxidation of SO_2 could have proceeded in a manner similar to that considered in this paper. Furthermore, the "activationless" nucleation mechanism may indeed be similar to the mechanism we have proposed here. Radical combination reactions such as reactions 16, 18, and 19 generally have zero activation energies. We feel, therefore, that the general idea embodied in the mechanism proposed here to explain nucleation with SO_2 is supported also by the findings of McMurry and Friedlander.[42]

G. Phenomenon of Photoinduced Nucleation. The experiments which formed the basis of this paper might be considered as being studies in the general class of photoinduced nucleation in which a mixture of gases, upon irradiation by light of a suitable wavelength, produces nuclei by the creation of an excited species. The excited species may interact with one or more of the original gaseous constituents, or they may react among themselves, or a combination of both types of reactions may occur. In the context of the mechanism proposed here for SO_2, N_2–O_2, H_2O mixtures, the excited species are O atoms, O_3, OH radicals plus SO_3, HSO_3, and HSO_5 radicals and their hydrates. The energy of the photons of irradiating light become transformed first to form O atoms (reaction 1) and then to form O_3 (reaction 2). Then the addition of light energy (of different wavelength) transforms O_3 into the excited species $O(^1D)$ (reaction 3) which then form OH (reaction 6) which forms $HSO_3 \cdot iH_2O$ (reactions 7 and 7′), etc. The reactions of the sulfur-bearing free radicals with each other represent the proposed actual nucleation steps. The energies of the absorbed photons are thus seen as producing reactive species, which through a series of exothermic reactions leads to the formation of nuclei.

The nucleation processes proposed by McMurry and Friedlander[42] may also be viewed in terms of the general system discussed above and in terms of the present notion of the chemical mechanism with their "monomers" being the excited species SO_3, HSO_3, HSO_5, and their hydrates, and the activationless nucleation process being the radical–radical reactions to form "polymers" (which are dimers). Recent publications by Katz et al.,[43] Wen et al.,[44] and Cordier and Papon[45] concern experiments on photoinduced nucleation in other systems, namely, nonane plus aldehydes,[43] H_2O,[44] and $CCl_4 + Cl_2$.[45] In the cases of nonane/aldehyde and CCl_4/Cl_2 it was shown that the nucleation was caused by excited species associated with the minor constituents—aldehydes and Cl_2. Cordier and Papon[45] demonstrated this quite clearly for CCl_4/Cl_2 and stated that "pure CCl_4 in the presence of light does not nucleate until supersaturation reaches its critical value; conversely one can initiate nucleation in the presence of Cl_2 at low concentration even at low supersaturation". Wen et al.[44] interpret their results in terms of a phenomenological model (for their thermal gradient diffusion cloud chamber) to conclude that nucleation was caused by electronically excited H_2O molecules. They state that they do not feel that nucleation could be caused by impurities since they were certain to be less than 1 ppm in the system. However, since the exciting wavelengths (200–320 nm) correspond to no known H_2O absorptions and in view of the discussion above concerning the work of Cordier and Papon,[45] the suspicion of impurities causing nucleation is still valid. We estimate crudely that as little as 1 ppb of a substance as reactive in the chamber of Wen et al.[44] as SO_2 was in the experiments of Leifer et al.[4] could have produced the nucleation observed (by Wen et al.[44]). In accordance with our model, we suggest that nucleation was caused by photolysis of a trace impurity followed by hydration of the resulting free radicals and then by radical–radical reactions.

In view of the above discussion we suggest that the general phenomenon of photoinduced nucleation, of which the SO_2 system studied in this paper is a special case probably having significance for atmospheric nucleation, can be explained by (1) the creation of free radicals by photolysis, (2) subsequent reactions of the radicals with gas-phase constituents to form the immediate nuclei precursors, and (3) a nucleation step which can be identified with a radical–radical combination (probably a quite general circumstance) or, as in the case of $SO_3 \cdot H_2O$, with an isomerization of a "mildly trapped" intermediate or activated molecular species.

V. Summary

Nucleation in a gaseous system in which SO_2 is photochemically oxidized is shown unlikely to be caused by the formation of large clusters of H_2SO_4 and H_2O molecules. But rather nucleation in such a system appears to be controlled by the kinetics of the photooxidation of SO_2. The chemical precursors of the nuclei are likely to be $SO_3 \cdot H_2O$ and HSO_3 and/or HSO_5 radicals in various states of hydration. The process of nucleation is apparently associated with the recombination of the HSO_3 and HSO_5 radicals (and hydrates) and a first-order process of $SO_3 \cdot H_2O$, which may be the isomerization to form H_2SO_4. A model set of elementary reactions is consistent with the above statements, and the calculated rates of nucleation generally fit the observed rates with reasonable values of reaction rate coefficients. On the basis of the model and simple gas kinetic theory, it is shown that the nuclei produced contain essentially a single stable sulfur molecule, such as $H_2S_2O_6$, $H_2S_2O_8$, SO_3, or H_2SO_4, and associated H_2O molecules. The results stand in rather dramatic contrast to the kinetic and critical cluster-size requirements of the theory of heteromolecular homogeneous nucleation of H_2SO_4 and H_2O mixtures.

Comparison of the results of this study with other experimentally oriented studies in nucleation shows that it is probable that the general phenomenon of photoinduced nucleation can be explained by initial formation of free radicals that, through a series of reactions, lead to the formation of nuclei via radical–radical combination reactions or an isomerization of a mildly trapped activated molecular species.

The findings of this paper are relevant to the understanding of processes by which particles may be formed in the atmosphere. A separate paper to assess the importance of those processes is under preparation. Further experimentation to provide more accurate estimates of

nucleation rates and their explicit dependencies upon SO_2, OH, O, and H_2O concentrations is currently in the preparatory phase.

Added Note. At the completion of this manuscript we became aware of a measurement of the equilibrium vapor pressure ($p^e_{H_2SO_4}$) by Roedel,[50] who found a value of 2.5×10^{-5} torr. This value is quite close to the value of 3.1×10^{-5} torr reported by Chu and Morrison[22] and used in this work.

Acknowledgment. The work reported in this paper was sponsored by the National Science Foundation under Grant No. ATM 76-00232. We are grateful to A. R. Bandy and A. L. Smith for useful discussions. We also gratefully acknowledge receiving helpful criticism from D. Stauffer and U. Brauner.

Appendix

From Table II the equations governing ozone are

$$O + O_2 + M \xrightarrow{k_2} O_3 + M$$

$$O_3 + h\nu \xrightarrow{j_3} O_2 + O(^1D)$$

$$O_3 + h\nu \xrightarrow{j_4} O_2 + O(^3P)$$

Therefore

$$\frac{d(O_3)}{dt} = k_2(O)(O_2)(M) - j_4(O_3) - j_3(O_3) \qquad (A1)$$

The solution of this differential equation yields (with (O) = a constant)

$$(O_3) = \frac{k_2(O)(O_2)(M)}{j_3 + j_4}(1 - e^{-(j_3+j_4)t}) \qquad (A2)$$

The characteristic time, τ, for developing a photochemical steady state in O_3 is $\tau = 1/(j_3 + j_4) = 662$ s. Since the average time of irradiation is estimated at 56 s, the O_3 concentrations must be considered as being governed by the condition

$$e^{-(j_3+j_4)t} \approx 1 - (j_3 + j_4)t$$

This, combined with the steady-state condition of O atoms

$$(O) = 2j_1/[k_2(M)]$$

gives

$$(O_3) = 2j_1(O_2)t \qquad (A3)$$

The production rate of X, the SO_2 oxidation products, is

$$Q = k_7(SO_2)(OH)[(M) + b(H_2O)] \qquad (A4)$$

This production rate, Q, is the sum of two production reactions for X, one with and one without water molecules as the third body. See the Discussion section, part D, especially eq 21 and 22, for a detailed description of these processes. The steady-state concentration of OH averaged over the irradiation zone can then be derived from the rates of reactions listed in Table II plus reaction 7′ to give

$$(OH) = \frac{2k_6j_3(H_2O)(O_3)}{[k_5(M) + k_6(H_2O)]k_7(SO_2)[(M) + b(H_2O)]} = \frac{4j_1j_3k_6(O_2)(H_2O)t}{[k_5(M) + k_6(H_2O)]k_7(SO_2)[(M) + b(H_2O)]} \qquad (A5)$$

If one substitutes eq A5 into eq A4 and notes that $k_6(H_2O) \ll k_5(M)$ in the experiments, the production rate of X becomes

$$Q = \frac{4k_6j_3j_1(O_2)(H_2O)t}{k_5(M)} \qquad (A6)$$

The ratio of SO_2 oxidation rates via O-atom attack to oxidation via OH attack, Γ, is given by

$$\Gamma = \frac{k_8(SO_2)(O)(M)}{k_7(SO_2)(OH)[(M) + b(H_2O)]} = \frac{k_8(O)(M)}{k_7(OH)[(M) + b(H_2O)]} \qquad (A7)$$

If one uses the relationship for oxygen-atom concentration (eq A3) and eq A5, along with the condition that $k_6(H_2O) \ll k_5(M)$, eq A7 can be manipulated to the form

$$\Gamma = t^{-1}\frac{k_5k_8(SO_2)}{k_2j_3k_6(O_2)}\frac{[(M) + b(H_2O)]}{(H_2O)} \qquad (A8)$$

When averaged over the irradiation zone, t is replaced by τ_r (=56 s). Thus in terms of experimental variables eq A8 becomes

$$\Gamma = E(H_2O)^{-1}[(M) + b(H_2O)] \qquad (A9)$$

where E is constant.

References and Notes

(1) A. Goetz and R. Pueschel, *Atmos. Environ.*, **1**, 287 (1967).
(2) J. Bricard, M. Cabane, G. Madelaine, and D. Vigla, *J. Colloid Interface Sci.*, **39**, 42 (1972).
(3) J. P. Friend, R. Leifer, and M. Trichon, *J. Atmos. Sci.*, **30**, 465 (1973).
(4) R. Leifer, J. P. Friend, and M. P. Trichon, *Proc. Int. Conf. Struct., Compos. Gen. Circ. Upper Lower Atmos. Possible Anthropogenic Perturbations*, 1974.
(5) C.-H. Shen and G. S. Springer, *Atmos. Environ.*, **10**, 235 (1976).
(6) M. Kasahara and K. Takahashi, *Atmos. Environ.*, **10**, 475 (1976).
(7) H. Reiss, D. C. Marvin, and R. H. Heist, *J. Colloid Interface Sci.*, **58**, 125 (1977).
(8) D. C. Marvin and H. Reiss, *J. Chem. Phys.*, **69**, 1897 (1978).
(9) F. E. Blacet, *Ind. Eng. Chem.*, **44**, 1339 (1952).
(10) W. A. Payne, L. J. Stief, and D. D. Davis, *J. Am. Chem. Soc.*, **95**, 7614 (1973).
(11) A. W. Castleman, Jr., R. E. Davis, H. R. Munkelwitz, I. N. Tang, and W. P. Wood, *Int. J. Chem. Kinet.*, Symp. 1, **7**, (1975).
(12) W. J. Shugard and H. Reiss, *J. Chem. Phys.*, **65**, 2827 (1976).
(13) C. S. Klang and D. Stauffer, *Faraday Symp. Chem. Soc.*, **7**, 26 (1973).
(14) W. A. Hoppel, *J. Rech. Atmos.*, **9**, 167 (1975).
(15) R. H. Heist and H. Reiss, *J. Chem. Phys.*, **61**, 573 (1974).
(16) P. Mirabel and J. L. Katz, *J. Chem. Phys.*, **60**, 1138 (1974).
(17) W. J. Shugard, R. H. Heist, and H. Reiss, *J. Chem. Phys.*, **61**, 5298 (1974).
(18) P. Hamill, C. S. Klang, and R. D. Cadle, *J. Atmos. Sci.*, **34**, 150 (1977).
(19) P. Mirabel and J. L. Clavelin, *J. Chem. Phys.*, **68**, 5020 (1978).
(20) J. I. Gmitro and T. Vermeulen, *AIChE J.*, **10**, 741 (1964).
(21) F. H. Verhoff and J. T. Banchero, *AIChE J.*, **18**, 1265 (1972).
(22) K. Chu and R. A. Morrison in "Environmental and Climatic Impact of Coal Utilization", J. J. Singh and A. Deepak, Eds., Academic Press, New York, 1980, p 293.
(23) E. N. Fuller, P. D. Schettler, and J. C. Giddings, *Ind. Eng. Chem.*, **58**, 19 (1966).
(24) W. Feller, "An Introduction to Probability Theory and Its Applications", 3rd ed., Wiley, New York, 1968.
(25) R. D. Hudson, *Can. J. Chem.*, **52**, 1456 (1974).
(26) "Chlorofluoromethanes and the Stratosphere", NASA Reference Publication 1010, Aug 1977.
(27) L. G. Anderson, *Rev. Geophys. Space Phys.*, **14**, 151 (1976).
(28) R. F. Hampson, Jr. and D. Garvin, Eds., *NBS Spec. Publ. (U.S.)*, **No. 513**, 1978.
(29) J. P. Burrows, G. W. Harris, and B. A. Thrush, *Nature (London)*, **267**, 233 (1977).
(30) J. L. Katz, *J. Chem. Phys.*, **52**, 4733 (1970).
(31) C. S. Klang, D. Stauffer, G. H. Walker, O. P. Puri, J. D. Wise, and E. M. Patterson, *J. Atmos. Sci.*, **28**, 1222 (1971).
(32) E. J. Hamilton and R. Lii, *Int. J. Chem. Kinet.*, **9**, 895 (1977).
(33) B. H. Y. Liu and C. S. Kim, *Atmos. Environ.*, **11**, 1097 (1977).
(34) D. D. Davis, A. R. Ravishankara, and S. Fischer, *Geophys. Res. Lett.*, **6**, 113 (1979).
(35) J. P. Friend, *Tellus*, **18**, 465 (1966).
(36) P. M. Holland and A. W. Castleman, Jr., *Chem. Phys. Lett.*, **56**, 511 (1978).
(37) R. A. Cox, *J. Phys. Chem.*, **76**, 814 (1972).

(38) E. R. Allen, R. D. McQuigg, and R. D. Cadle, *Chemosphere*, **1**, 25 (1972).
(39) R. A. Cox, *Aerosol Sci.*, **4**, 473 (1973).
(40) R. Smith, R. G. DePena, and J. Heicklen, *J. Colloid Interface Sci.*, **53**, 202 (1975).
(41) P. A. Leighton, "Photochemistry of Air Pollution", Academic Press, New York, 1961.
(42) P. M. McMurry and S. K. Friedlander, *J. Colloid Interface Sci.*, **64**, 248 (1978).
(43) J. L. Katz, F. C. Wen, T. McLaughlin, R. J. Reusch, and R. Partch, *Science*, **196**, 1203 (1977).
(44) F. C. Wen, T. McLaughlin, and J. L. Katz, *Science*, **200**, 769 (1978).
(45) B. Cordier and P. Papon, *Chem. Phys. Lett.*, **59**, 113 (1978).
(46) It has been suggested that the H_2O vapor added to the reactor could affect the efficiency of the CN counter. Because the counter operates by raising the relative humidity of the sampled gas to 100% before the induction of nucleation, the amount of water vapor in the sample should have a minimal effect, if any, upon the efficiency of the counter. Rather, it is evident that the added H_2O affected the creation of nuclei in the flow reactor.
(47) Later in the paper an additional, different reaction of OH with SO_2 is postulated which results in the concentrations listed in column 4b. However, because of the necessity that the OH concentration must be determined by a steady state of production, the quantities (X) and the rate of SO_2 loss are unaffected by the differences in (OH).
(48) The activity of a substance is the ratio of its vapor pressure to its equilibrium vapor pressure over the pure liquid. It is the generalization of relative humidity.
(49) By multiplicative fractional error we mean that fraction, ϵ, which mean divided into the expected value gives the lower limit of the confidence interval and when multiplied by the expected value gives the upper limit of the confidence interval. With $\langle Q \rangle$ as the expected value we may write $\langle Q \rangle/\epsilon \leq Q \leq \langle Q \rangle\epsilon$.
(50) W. Roedel, *J. Aerosol. Sci.*, **10**, 375 (1979).

Transfer of Hydrogen by Hydroaromatics. 1. Mechanism of Dehydrogenation/Hydrogenation in Tetralin/Iron Catalyst Systems

T. Gangwer

Chemical Sciences Division, Department of Energy and Environment, Brookhaven National Laboratory, Upton, New York 11973
(Received: July 16, 1979; In Final Form: March 12, 1980)

At 400 °C, the gas-phase dehydrogenation of tetralin over iron catalysts is found to result in formation of naphthalene via the reaction of intermediate 1,2-dihydronaphthalene. The kinetic data for these systems were found to follow heterogeneous, first-order rate laws. A mechanism is presented which quantitatively describes the measured tetralin and naphthalene kinetic behavior and successfully predicts the kinetic data observed for the 1,2-dihydronaphthalene intermediate. The rate-limiting reactions in these systems are proposed as involving dehydrogenation/hydrogenation reactions on the surfaces of the catalysts. Based on the data analysis, the rate constants for the surface reactions have values in the 10^{-4}–10^{-5}-s^{-1} range. The catalytic surface site populations were found to be in the range 10^{13}–10^{14} molecules cm^{-2}.

Introduction

The hydrogen-transferring property of hydroaromatics—in particular, tetralin systems—has been the subject of investigation by various researchers.[1-4] These investigations have focused on product identification and the effect of substituents on product composition. The tetralin dehydrogenation/hydrogenation process has been characterized in terms of material balance reaction schemes. Recent investigation of the gas-phase kinetics and the mechanism of tetralin hydrogen-transfer chemistry at 400 °C found the rate-limiting steps to be heterogeneous, zero-order reactions in the absence of added catalysts.[5]

Chemical donation of hydrogen via hydroaromatic molecules such as tetralin to organic molecules undergoing thermal bond cleavage results in formation of lower molecular weight products.[6,7] Such hydrogenation chemistry forms the basis of numerous coal liquefaction processes. Investigation of the mechanisms (both catalytic and noncatalytic) by which hydroaromatics transfer hydrogen is an ongoing effort at this laboratory. The present paper reports the kinetic results obtained when tetralin gas was reacted at 400 °C over iron oxide and iron sulfide catalysts. A general mechanism is presented which quantitatively characterizes these catalytic systems.

Experimental Section

The tetralin, obtained from Aldrich Chemical, was 99.4% pure (the main impurity being 0.4% naphthalene) and was used as received. The iron(III) oxide (Fe_2O_3) was from the Baker Chemical Co. The limonite ($2Fe_2O_3 \cdot 3H_2O$), magnetite (Fe_3O_4), and pyrite (FeS_2) catalysts were purchased from Ward's Scientific Co. The catalysts were ground and sieved such that only those solids which were ~44 μm or less were used.

The reaction vessels were 10-cm long quartz tubes (16.0-mm diameter). The catalysts (100 mg unless noted otherwise) were degassed on a vacuum line at room temperature by pumping on the quartz vessel until the system pressure fell below 10^{-5} torr (15–20 min pumping time). Degassed organics (100 μL unless noted otherwise) were then vacuum distilled onto the minerals, and the quartz tubes were sealed. The transfer efficiency for the vacuum distillations was determined to be 89.9 ± 0.6%. The vessels were placed in a 400 °C oven for the required period of time, removed, and rapidly chilled to room temperature by plunging into water. The oven interior was a large heat sink (10-kg steel block) with four concentric 18-mm diameter by 12-cm deep chambers for the reaction vessels. The reaction vessel interior reached 400 °C within 5 min and had a 2 °C axial gradient at 400 °C.

The product mixtures were extracted from the vessels by washing with 0.5 mL of analytical grade benzene and analyzed on a Hewlett Packard Model 5750 gas chromatograph by using the flame ionization detector and dual 6-ft Durapak (Carbowax 400-Porasil F) $^1/_8$-in. columns. The GC data were analyzed by using a Hewlett-Packard integrator and are reported as area percent. The tetralin and naphthalene analyses were reproducible to within 1% of the reported area percent values. The 1,2-dihydronaphthalene analysis was not as reproducible (12% of the observed area percent values) because this species eluted on the shoulder of the much larger tetralin peak.

Results

The gas-chromatographic analyses showed that the main products of the tetralin dehydrogenation were 1,2-di-

0022-3654/80/2084-2436$01.00/0